

Patterning Graphene through the Self-Assembled Templates: Toward Periodic Two-Dimensional Graphene Nanostructures with Semiconductor Properties

Alexander Sinitskii[†] and James M. Tour^{*,†,‡}

Departments of Chemistry, Computer Science, Mechanical Engineering and Materials Science, and Smalley Institute for Nanoscale Science and Technology, Rice University, MS 222, 6100 Main Street, Houston, Texas 77005

Received June 21, 2010; E-mail: tour@rice.edu

Abstract: Periodic graphene nanostructures are fabricated via patterning graphene through the self-assembled monolayers of monodisperse colloidal microspheres. The resulting structures exhibit promising electronic properties featuring high conductivities and ON–OFF ratios up to 10. The apparent advantages of the presented method are the possibilities of fabricating periodic graphene nanostructures with different periodicities, ranging from ~100 nm to several μm , and also varying the periodicity and the neck width independently. The use of the presented method yields graphene nanostructures with variable electronic properties.

Since the isolation of graphene in 2004,¹ there has been considerable interest in graphene nanostructures with feature sizes less than 10 nm since they were theoretically² and experimentally^{3,4} shown to have electronic band gaps large enough for room temperature transistor operation. Such graphene nanostructures, nanoribbons³ and quantum dots,⁴ were first fabricated by a combination of electron beam (e-beam) lithography and dry etching. However, patterning sub-10-nm-wide graphene nanoribbons (GNRs) by e-beam lithography is still quite challenging and requires state-of-the-art experimental facilities. Therefore, alternative techniques for making GNRs, including a solution-based approach,⁵ unzipping of carbon nanotubes,^{6–8} and masking graphene with silicon nanowires (SiNWs),⁹ were recently developed. Using SiNWs is interesting in the sense that the masks for making the narrow GNRs became available not through state-of-the-art top-down fabrication procedures but through relatively simple chemistry since the growth of SiNWs is a well-developed area of materials science.¹⁰

Recently, another bottom-up approach was developed for making graphene nanostructures with sub-10-nm features: patterning graphene via block copolymer lithography.^{11,12} The resulting graphene nanostructures, dubbed ‘graphene nanomeshes’ (GNMs), are schematically shown in the inset in Figure 1a. They may possess an electronic band gap if the neck width (w) is small enough and, thus, exhibit ON–OFF ratios comparable to those previously achieved in individual GNR devices. But at the same time these GNMs can support currents that are orders of magnitude higher than those typically reported for the GNR devices. Since the GNMs have these unique characteristics, further research on these graphene nanostructures is in order. In addition to the semiconductor properties, unusual physical phenomena may be anticipated for these highly periodic graphene structures, especially if the values of the neck width (w) and periodicity (d) could be independently tuned over a wide range.

We report here an alternative approach for making large-scale GNMs, which is based on patterning graphene using self-assembled

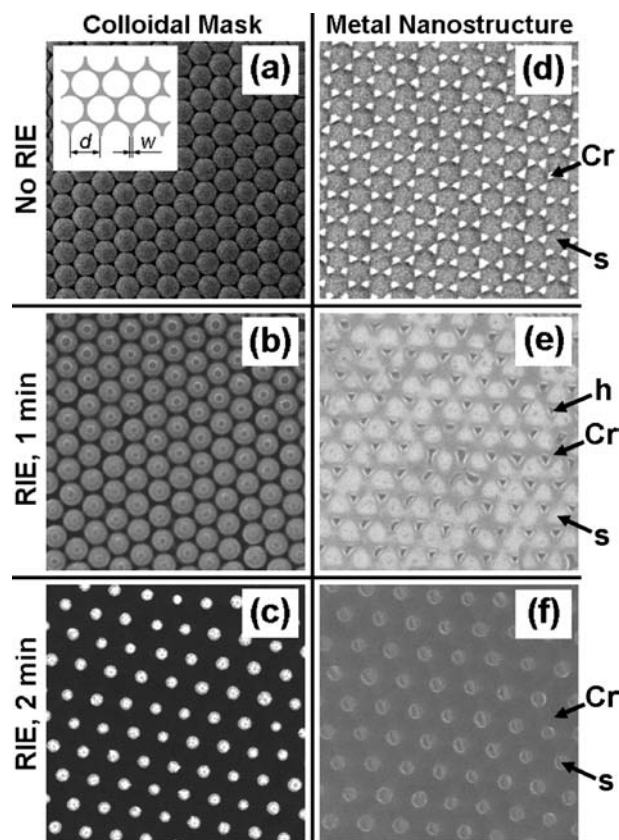


Figure 1. Using RIE for defining different periodic metallic nanostructures in nanosphere lithography as viewed by scanning electron microscopy (SEM). (a) A monolayer of monodisperse silica microspheres with an average diameter of ~400 nm on a Si/SiO₂ substrate. The inset shows a schematic for a GNM, where d is the periodicity of the structure and w is the neck width. (b, c) Similar monolayers after 1 and 2 min of CF₄ RIE, respectively. (d, e, f) Metal nanostructures obtained by depositing 70 nm of Cr on the substrate (a) and 10 nm of Cr on the substrates (b and c), respectively, followed by removing the silica microspheres. Arrows show the substrate (s) visible through the Cr nanostructure and holes (h) in the substrate caused by RIE.

monolayers of monodisperse colloidal microspheres. While block copolymer lithography is a powerful tool for making nanostructures with sub-100-nm periodicity,¹³ monodisperse colloidal microspheres with an average size ranging from 100 nm to several μm are readily available commercially or through well-established chemistries.¹⁴ Therefore, these two approaches can be considered complementary in terms of achieving GNMs with different periodicities, since using colloidal microspheres instead of block copolymers enables covering almost 2 additional orders of magnitude of d . Furthermore, self-assembly of colloidal microspheres has been studied for decades, for purposes ranging from the modeling of the phase transitions in

[†] Department of Chemistry.

[‡] Departments of Computer Science, Mechanical Engineering and Materials Science, and Smalley Institute for Nanoscale Science and Technology.

solids¹⁵ to the synthesis of photonic crystals¹⁶ and ordered nanostructures.¹⁷ Therefore, different approaches for growing high-quality large-scale monolayers of colloidal spheres, such as convective self-assembly,¹⁸ electrophoretic deposition,¹⁹ ordering in the confinement cells,²⁰ and others,²¹ are already developed and thus can be immediately exploited for making GNMs. Finally, we demonstrate that the new approach enables independently tuning w and d in the GNMs; d is determined by the size of colloidal microspheres and w is controlled by the etching duration, thus making this approach attractive for fabricating GNMs with different geometric characteristics. Importantly, the electronic properties of GNMs have been theoretically shown to depend on both d and w .²²

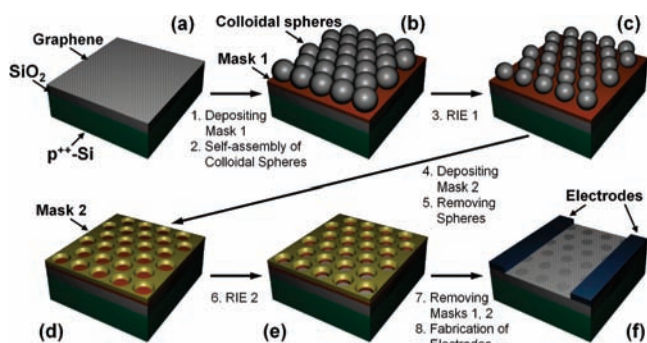


Figure 2. Scheme for the fabrication of GNMs; see text for details.

The key step in producing GNMs using colloidal microspheres is making a periodic porous mask for etching graphene. For this purpose we used an approach that can be defined as modified nanosphere lithography. In conventional nanosphere lithography, periodic arrays of colloidal particles are used as the mask for depositing separated nanoparticles; see the top row images in Figure 1. Here, we introduce an additional reactive ion etching (RIE) step to form gaps between the close-packed colloidal spheres. In this case, if masking material is deposited on the substrate and the spheres are selectively removed, a continuous mask rather than an array of separated nanoparticles is formed on the surface. By changing the duration of the RIE, the size of these gaps and therefore the width of the necks in the resulting mask for etching graphene can be finely tuned over a wide range, as illustrated by Figure 1b,e and 1c,f.

The structure shown in Figure 1e could be an ideal etch mask for making GNMs. However, triangular holes in the Si/SiO₂ substrate, which were caused by the RIE process, are evident. To protect the graphene from this etching, which is intended to affect the colloidal spheres only, a protective layer between graphene and colloidal spheres was introduced; this layer is referred to as Mask 1. All of the fabrication steps for making GNMs are shown in Figure 2 and described in detail in Experimental Details. We note that this approach is versatile, as different combinations of the mask materials and etching procedures, as well as different colloidal spheres and different approaches for their assembly and removal, can be used. In this work we used silica spheres made using Stöber's method,²³ although the procedure can be easily adjusted for using other monodisperse spheres, such as polystyrene beads,²⁴ that are also often used in materials research. We used SiO₂ as Mask 1 and Au as Mask 2, and both RIE steps used CF₄ as the etching gas (in the RIE 2 it was mixed with O₂). The colloidal spheres were deposited on the substrates by convective self-assembly^{18c} and removed by ultrasonication in a water bath.

To demonstrate that GNMs with different periodicities can be fabricated according to the procedure shown in Figure 2, we synthesized three suspensions of monodisperse silica microspheres

with an average diameter of ~ 110 , ~ 270 , and ~ 400 nm. According to the SEM results, in each case the standard deviation of sizes was $<5\%$ (at least 100 spheres of each type were sized). Large ($\sim 1 \times 1$ cm²) graphene films for patterning were synthesized by the high-temperature decomposition of methane on copper foils and then transferred to Si/SiO₂ substrates.²⁵

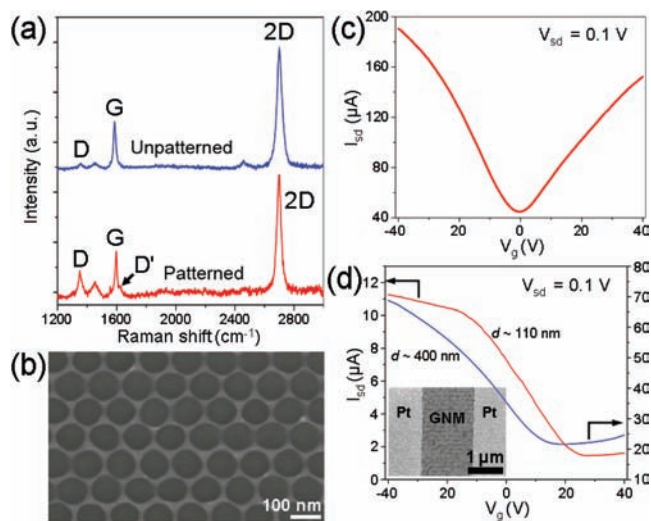


Figure 3. Graphene properties before and after patterning. (a) Typical Raman spectra of the unpatterned and patterned graphene areas on the same substrate. (b) SEM image of a GNM patterned using 110-nm-sized silica particles. (c) Transfer characteristics of the as-prepared graphene film. The device channel has a width of 1 μm and a length of 2 μm. (d) Transfer characteristics of GNM devices of similar dimensions (width = 20 μm, length = 1.5 μm) patterned using silica particles that have an average diameter of 110 nm (red) and 400 nm (blue). The inset shows an SEM image of a fragment of the device patterned using 110-nm-sized silica particles.

After the patterning we performed Raman spectroscopy studies of the unpatterned and patterned graphene areas on the same substrate (Figure 3a). Raman spectra of the unpatterned areas show that the synthesized graphene films were mostly monolayers with a less than 1:2 G-to-2D intensity ratio, and a symmetric 2D band was centered at ~ 2690 cm⁻¹ with a full width at half-maximum of ~ 35 cm⁻¹.²⁶ For different areas of the unpatterned graphene we observed only tiny or no D band, and no D' band. In contrast, in the patterned areas, both D and D' bands were clearly observed; these are due to a high percentage of the edge atoms in GNMs.²⁷ In the GNMs with $w < 20$ nm, the intensity of the D band is comparable to or higher than that of the G band.

Figure 3b shows an SEM image of the GNM obtained by masking graphene using 110-nm silica particles. This image demonstrates that narrow ($w < 20$ nm) necks in the GNM are attainable using the described procedure. Similar SEM images were recorded for the GNMs with other periodicities. In order to fabricate such GNMs, we used an aggressive overetching RIE 2 in addition to the well-controlled RIE 1, which, however, resulted in the breakage of some of the narrower necks. Importantly, recently developed techniques for graphene growth on the metal surfaces allow for making extremely large graphene films; samples up to several cm² have been reported.^{25,28} Similarly, monodisperse colloidal particles, such as silica microspheres, can be synthesized in large quantities from inexpensive reagents (for instance, silica spheres are synthesized through the hydrolysis of tetraethyl orthosilicate²³) and then their macroscopic ensembles can be fabricated. Therefore, graphene grown on metal substrates, combined with colloidal spheres as the masks, potentially enables making macroscopic GNMs that could be attractive as optically transparent films with tunable (depending on w - and d -values) electronic properties. We note

though that in the present work we did not succeed in making ultralarge GNMs with defect-free structures (i.e., an enlarged area that has the nearly perfect regularity demonstrated in Figure 3b), because the self-assembly of colloidal particles inevitably results in the formation of various defects such as vacancies, holes, and domain boundaries. However, we did observe some GNM domains with an area of a few tens of μm^2 with little or almost no defects. The size of such areas may be further improved by employing better techniques for the colloidal particle self-assembly.

Figure 3c illustrates the electrical properties of a typical electronic device made from an unpatterned monolayer film. This device exhibits an ambipolar electric field effect typical for graphene with mobilities of 870 and 560 $\text{cm}^2/\text{V}\cdot\text{s}$ for holes and electrons, respectively; these values are comparable to those previously reported for graphene grown on metallic substrates.^{25,28} Most importantly, the electronic properties of graphene change dramatically after the patterning. Figure 3d shows two typical transfer characteristics recorded for the GNMs with $d = 110$ and 400 nm and sub-20-nm necks. The GNM devices (see the inset) show a p-type transistor behavior instead of an ambipolar electric field effect. This hole doping is similar to that previously reported for GNR devices^{3,5,9} and most likely caused mainly by the edge oxidation of the GNMs during the O_2 RIE 2; physisorbed species may also contribute to this doping effect.²⁹ The $I_{\text{sd}}-V_{\text{g}}$ plot also shows that the device with $d = 110$ nm has an ON-OFF ratio of ~ 8 , which is comparable to GNR field-effect transistors with widths ~ 15 nm.^{3,5,9} As an example of a GNM with another periodicity, shown is the device with $d = 400$ nm that exhibits a lower ON-OFF ratio of ~ 2.5 . Some GNM devices exhibited ON-OFF ratios up to 10. Further optimization of the synthetic procedure should result in GNMs with narrower necks and thus higher ON-OFF ratios. The energy gap in GNMs can be estimated using the model described in ref 22. According to this model, a GNM with $d = 110$ nm and $w = 15$ nm should have an energy gap of ~ 0.05 eV. It is also interesting that, for the GNMs with the same w , the energy gap size decreases with increasing d .²²

In conclusion, we have demonstrated a simple, tunable, and potentially scalable method for patterning graphene. The resulting GNMs exhibit promising electronic properties featuring high conductivities and ON-OFF ratios. The apparent advantages of the present method are the possibilities of fabricating GNMs with different periodicities, ranging from ~ 100 nm to several μm , and also varying the periodicity of the GNM and the neck width independently, which should result in graphene nanostructures with different electronic properties.

Experimental Details. Fabrication of GNMs. Graphene was grown according to the reported procedure²⁵ and then transferred onto heavily doped p-type Si substrates with a 200 nm thermal SiO_2 layer (SQI). Silica colloidal microspheres were synthesized by the Stöber method.²³ Mask 1 (SiO_2 , 10 nm) was deposited on graphene-covered Si/ SiO_2 substrates by PE-CVD, and then monolayers of colloidal spheres were formed by self-assembly on a vertical substrate.^{18c} RIE 1 (CF_4) was used to define ~ 10 nm gaps between the spheres; the smaller the size of colloidal spheres, the shorter the time that is required. Mask 2 (Au, 10 nm) was deposited by e-beam evaporation, and then the colloidal spheres were removed by intense ultrasonication in water. In the RIE 2 step we mixed CF_4 with O_2 (1:1) to remove the graphene. Both Masks 1 and 2 were then removed by short etching with dilute HF. Fabrication of graphene and GNM devices was performed by two-step e-beam lithography. In a first step, PMMA was patterned into 1–20 μm wide strips on top of graphene or large-scale GNM to define the device channels, then the unprotected material was etched away by O_2 plasma, and then the remaining PMMA was dissolved in acetone. In a second step, 20-nm-thick Pt contacts were placed

across the resulting graphene or GNM strips by e-beam lithography followed by e-beam evaporation.

Sample Analysis. SEM imaging was performed on a JEOL-6500 field-emission microscope. Raman spectroscopy was performed on a Renishaw Raman microscope using a 514 nm laser. The electrical transport properties were tested using a probe station (Desert Cryogenics TT-probe 6 system) under vacuum with the chamber base pressure below 10^{-5} Torr. The IV data were collected by an Agilent 4155C semiconductor parameter analyzer.

Acknowledgment. This work was supported by the AFRL through University Technology Corporation, 09-S568-064-01-C1, the AFOSR FA9550-09-1-0581, and the ONR MURI Program.

References

- (1) Novoselov, K. S.; Geim, A. K.; Morozov, S. V.; Jiang, D.; Zhang, Y.; Dubonos, S. V.; Grigorieva, I. V.; Firsov, A. A. *Science* **2004**, *306*, 666.
- (2) (a) Son, Y. W.; Cohen, M. L.; Louie, S. G. *Phys. Rev. Lett.* **2006**, *97*, 216803. (b) Barone, V.; Hod, O.; Scuseria, G. E. *Nano Lett.* **2006**, *6*, 2748.
- (3) (a) Han, M. Y.; Özyilmaz, B.; Zhang, Y.; Kim, P. *Phys. Rev. Lett.* **2007**, *98*, 206805. (b) Chen, Z.; Lin, Y. M.; Rooks, M. J.; Avouris, P. *Physica E* **2007**, *40*, 228.
- (4) Ponomarenko, L. A.; Schedin, F.; Katsnelson, M. I.; Yang, R.; Hill, E. W.; Novoselov, K. S.; Geim, A. K. *Science* **2008**, *320*, 356.
- (5) Li, X.; Wang, X.; Zhang, L.; Lee, S.; Dai, H. *Science* **2008**, *319*, 1229.
- (6) (a) Kosynkin, D. V.; Higginbotham, A. L.; Sinititskii, A.; Lomeda, J. R.; Dimiev, A.; Price, B. K.; Tour, J. M. *Nature* **2009**, *458*, 872. (b) Sinititskii, A.; Fursina, A. A.; Kosynkin, D. V.; Higginbotham, A. L.; Natelson, D.; Tour, J. M. *Appl. Phys. Lett.* **2009**, *95*, 253108. (c) Higginbotham, A. L.; Kosynkin, D. V.; Sinititskii, A.; Sun, Z.; Tour, J. M. *ACS Nano* **2010**, *4*, 2059.
- (7) (a) Jiao, L.; Zhang, L.; Wang, X.; Diankov, G.; Dai, H. *Nature* **2009**, *458*, 877. (b) Jiao, L.; Wang, X.; Diankov, G.; Wang, H.; Dai, H. *Nat. Nanotechnol.* **2010**, *5*, 321.
- (8) Cano-Márquez, A. G.; Rodríguez-Macías, F. J.; Campos-Delgado, J.; Espinosa-González, C. G.; Tristán-López, F.; Ramírez-González, D.; Cullen, D. A.; Smith, D. J.; Terrones, M.; Vega-Cantú, Y. I. *Nano Lett.* **2009**, *9*, 1527.
- (9) Bai, J.; Duan, X.; Huang, Y. *Nano Lett.* **2009**, *9*, 2083.
- (10) Lu, W.; Lieber, C. M. *J. Phys. D: Appl. Phys.* **2006**, *39*, R387.
- (11) Bai, J.; Zhong, X.; Jiang, S.; Huang, Y.; Duan, X. *Nat. Nanotechnol.* **2010**, *5*, 190.
- (12) Kim, M.; Safron, N. S.; Han, E.; Arnold, M. S.; Gopalan, P. *Nano Lett.* **2010**, *10*, 1125.
- (13) Kim, H. C.; Park, S. M.; Hinsberg, W. D. *Chem. Rev.* **2010**, *110*, 146.
- (14) Xia, Y.; Gates, B.; Yin, Y.; Lu, Y. *Adv. Mater.* **2000**, *12*, 693.
- (15) (a) Pusey, P. N.; van Meegen, W. *Nature* **1986**, *320*, 340. (b) Zhu, J.; Li, M.; Rogers, R.; Meyer, W.; Ottewill, R. H.; STS-73 Space Shuttle Crew; Russel, W. B.; Chaikin, P. M. *Nature* **1997**, *387*, 883.
- (16) (a) Stein, A. *Microporous Mesoporous Mater.* **2001**, *44–45*, 227. (b) López, C. *Adv. Mater.* **2003**, *15*, 1679.
- (17) (a) Haynes, C. L.; Van Duyne, R. P. *J. Phys. Chem. B* **2001**, *105*, 5599. (b) Kosiorek, A.; Kandulski, W.; Chudzinski, P.; Kempa, K.; Giersig, M. *Nano Lett.* **2004**, *4*, 1359. (c) Sinititskii, A.; Neumeier, S.; Nelles, J.; Fischler, M.; Simon, U. *Nanotechnology* **2007**, *18*, 305307.
- (18) (a) Denkov, N. D.; Velez, O. D.; Kralchevsky, P. A.; Ivanov, I. B.; Yoshimura, H.; Nagayama, K. *Langmuir* **1992**, *8*, 3183. (b) Dimitrov, A. S.; Dushkin, C. D.; Yoshimura, H.; Nagayama, K. *Langmuir* **1994**, *10*, 432. (c) Dimitrov, A. S.; Nagayama, K. *Langmuir* **1996**, *12*, 1303.
- (19) (a) Giersig, M.; Mulvaney, P. *Langmuir* **1993**, *9*, 3408. (b) Zhang, K. Q.; Liu, X. Y. *Nature* **2004**, *429*, 739.
- (20) Park, S. H.; Qin, D.; Xia, Y. *Adv. Mater.* **1998**, *10*, 1028.
- (21) (a) Im, S. H.; Lim, Y. T.; Suh, D. J.; Park, O. O. *Adv. Mater.* **2002**, *14*, 1367. (b) Kim, M. H.; Im, S. H.; Park, O. O. *Adv. Funct. Mater.* **2005**, *15*, 1329. (c) Mihi, A.; Ocaña, M.; Míguez, H. *Adv. Mater.* **2006**, *18*, 2244.
- (22) Pedersen, T. G.; Flindt, C.; Pedersen, J.; Mortensen, N. A.; Jauho, A. P.; Pedersen, K. *Phys. Rev. Lett.* **2008**, *100*, 136804.
- (23) (a) Stöber, W.; Fink, A.; Bohn, E. *J. Colloid Interface Sci.* **1968**, *26*, 62. (b) Bogush, G. H.; Tracy, M. A.; Zukoski, C. F. *J. Non-Cryst. Solids* **1988**, *104*, 95. (c) Hartlen, K. D.; Athanopoulos, A. P. T.; Kitaev, V. *Langmuir* **2008**, *24*, 1714–1720.
- (24) Goodwin, J. W.; Hearn, J.; Ho, C. C.; Ottewill, R. H. *Colloid Polym. Sci.* **1974**, *252*, 464.
- (25) Li, X.; Cai, W.; An, J.; Kim, S.; Nah, J.; Yang, D.; Piner, R.; Velamakanni, A.; Jung, I.; Tutuc, E.; Banerjee, S. K.; Colombo, L.; Ruoff, R. S. *Science* **2009**, *324*, 1312.
- (26) Ferrari, A. C.; Meyer, J. C.; Scardaci, V.; Casiraghi, C.; Lazzeri, M.; Mauri, F.; Piscanec, S.; Jiang, D.; Novoselov, K. S.; Roth, S.; Geim, A. K. *Phys. Rev. Lett.* **2006**, *97*, 187401.
- (27) Gupta, A. K.; Russin, T. J.; Gutiérrez, H. R.; Eklund, P. C. *ASC Nano* **2009**, *3*, 45.
- (28) Reina, A.; Jia, X.; Ho, J.; Nezich, D.; Son, H.; Bulovic, V.; Dresselhaus, M. S.; Kong, J. *Nano Lett.* **2009**, *9*, 30.
- (29) Schedin, F.; Geim, A. K.; Morozov, S. V.; Hill, E. W.; Blake, P.; Katsnelson, M. I.; Novoselov, K. S. *Nat. Mater.* **2007**, *6*, 652.

JA105426H